



HAL
open science

Determination of the random anisotropic elasticity layer using transient wave propagation in a fluid-solid multilayer: Model and experiments

Christophe Desceliers, Christian Soize, Q. Grimal, M. Talmant, S. Naili

► To cite this version:

Christophe Desceliers, Christian Soize, Q. Grimal, M. Talmant, S. Naili. Determination of the random anisotropic elasticity layer using transient wave propagation in a fluid-solid multilayer: Model and experiments. *Journal of the Acoustical Society of America*, 2009, 125 (4), pp.2027-2034. 10.1121/1.3087428 . hal-00684450

HAL Id: hal-00684450

<https://hal.science/hal-00684450v1>

Submitted on 2 Apr 2012

HAL is a multi-disciplinary open access archive for the deposit and dissemination of scientific research documents, whether they are published or not. The documents may come from teaching and research institutions in France or abroad, or from public or private research centers.

L'archive ouverte pluridisciplinaire **HAL**, est destinée au dépôt et à la diffusion de documents scientifiques de niveau recherche, publiés ou non, émanant des établissements d'enseignement et de recherche français ou étrangers, des laboratoires publics ou privés.

Identification of an anisotropic elasticity tensor for an elastic layer using transient wave propagation in a fluid-solid multilayer – Model with uncertainties and Experiments

Christophe Desceliers^{a)} and Christian Soize^{b)}

*Université Paris-Est, Modélisation et Simulation Multi Echelle, FRE3160 CNRS,
5 bd Descartes, 77454 Marne-la-Vallée, France*

Quentin Grimal^{c)} and Maryline Talmant^{d)}

*Université Paris VI, Laboratoire d'Imagerie Paramétrique, UMR CNRS 7623,
15 rue de l'école de médecine, 75006 Paris, France*

Salah Naili^{e)}

*Université Paris-Est, Laboratoire de Mécanique Physique, UMR CNRS 7052 B2OA,
61 avenue du Général de Gaulle, 94010 Creteil Cedex, France*

(Dated: February 18, 2008)

The aim of this paper is to introduce a simplified model useful for the ultrasonic characterization of a solid with uncertain elastic behavior. The model consists of a solid layer sandwiched between two acoustic fluid layers and an acoustic source placed in one fluid layer. Uncertainties are taken into account with a probabilistic model of the elasticity tensor. Its parameters are the mean value of the random tensor and a coefficient δ that controls the statistical fluctuation level. The characterization of the solid layer given a database of actual measurements consists in the identification of the (i) elastic parameters of the mean elasticity model; (ii) coefficient δ ; and (iii) mass density. This is performed with a numerical solver of wave propagation. The model is representative of measurements of human bone properties with the so-called axial transmission technique. The identification was conducted for *in vivo* data collected previously. The capability of the model to predict the velocity of the first experimental arriving signal in the statistical sense is proved. The identified anisotropic elasticity tensor of cortical bone from actual data based on the simplified model is given.

PACS numbers: 20

I. INTRODUCTION

Elastic wave propagation can be used to characterize the anisotropic elasticity tensor of solids. For highly heterogeneous materials (e.g. concrete, wood, soft tissue, bone, etc.) not only the values of the stiffness constants may vary within the tested structure but also the material symmetry. For biological materials this is basically a consequence of their multi-scale organization and of significant variations of the constitution at the nanoscopic scales. When the length scale of the heterogeneities is larger or of the order of magnitude of the wavelength, the determination of the elastic properties with acoustic waves is a challenge. If the acoustic signals used for material characterization have a large amount of scatter, the elastic tensor may be considered as not unique: the probed elastic properties depend on the actual wave path inside the material. In this context, the problem of elasticity identification may advantageously be formulated as the determination of a mean elasticity tensor and of

the fluctuations of the elasticity around the mean tensor. In other words, since any model useful for the elasticity identification is always a rough approximation of the reality, the modeling of uncertainties may be considered in order to extend the domain of validity of the model.

The aim of this paper is to introduce a simplified elasto-acoustic model useful for the ultrasonic characterization of a solid layer with uncertain elastic behavior. The identification of the material properties of an elastic layer that represents a human compact bone is considered. However the method developed is of a wider interest as it may be applied straightforward to the characterization of other materials. The model is representative of an *in vivo* measurement of bone properties with the so-called axial transmission technique. The point is to investigate whether the proposed wave propagation model including a stochastic model of bone anisotropic elastic properties is able to account for *in vivo* measurements in a statistical sense. Thus, if it is possible to find the parameters of a stochastic model whose response has the same statistical properties as the *in vivo* measurements database, then the model may be a good candidate to solve stochastic inverse problems and determine bone elastic properties.

The axial transmission technique provides the velocity of ultrasonic waves axially transmitted along compact (cortical) bone through a linear arrangement of emitters and receivers placed on the same side of the skeletal site.

^{a)}Electronic address: christophe.desceliers@univ-paris-est.fr

^{b)}Electronic address: christian.soize@univ-paris-est.fr

^{c)}Electronic address: quentin.grimal@lip.bhdc.jussieu.fr

^{d)}Electronic address: talmant@lip.bhdc.jussieu.fr

^{e)}Electronic address: naili@univ-paris12.fr

This technique has been extensively used to probe bone quality at the radius (see Bossy *et al.* (2004a); Camus *et al.* (2000)). In particular, the bidirectional axial transmission technique associated with a measurement of the velocity of the first arriving contribution of the signal (FAS) is a technique sensitive to the elasticity of radius cortical bone. Bossy *et al.* (2004b,c); Grimal *et al.* (2007); Raum *et al.* (1999) also suggest that bone mass density and bone thickness are other less important determinants of the FAS. Accordingly, as a matter of simplification, thickness will be considered as fixed in this work and density will be taken as a deterministic varying parameter which has to be identified as well as the elastic properties. For the purposes of the present work, experimental data previously collected with a bidirectional axial transmission device could be used to investigate the possible determination of compact bone stiffness tensor.

The simplified elasto-acoustic model is a three-layers system: a solid layer sandwiched between two inviscid acoustic fluid layers. The elastic layer (cortical bone) is a homogeneous anisotropic elastic material while the fluid (acoustic) layers represent soft tissues. The uncertainties on the elasticity of bone are introduced *via* a probabilistic approach developed in Soize (2001, 2005). It should be noted that a first application of the parametric probabilistic approach to the axial transmission technique can be found in Macocco *et al.* (2006). The parameters of the probabilistic model are the mean value of the random elasticity tensor and an additional parameter that controls the statistical fluctuation level. The mean model for bone is transversely isotropic and the uncertain fluctuations are anisotropic.

The identification of the parameters of the algorithm of the model, including the parameters of the probabilistic model, is formulated as an optimization problem. The algorithm used to calculate the values of the cost function for several test values of the parameters of the stochastic model is performed by means of a stochastic solver based on the Monte Carlo method associated with a hybrid numerical solver of wave propagation presented in Desceliers *et al.* (2008): for each independent realization of the random effective elasticity tensor, the transient elasto-acoustic response is calculated by the wave propagation solver.

The capability of the stochastic model to represent the elasto-acoustic response of the uncertain system is demonstrated by a comparison of the model output to a database of *in vivo* measurements. In order to obtain a rich database from the statistical point of view, measurements from 168 patients were pooled; then the database takes into account of a large variability of the properties of the elasto-acoustic system under consideration. Finally, the validation of the model consists in the comparison of the statistical properties of the model response to those of the *in vivo* measurements. Once validated, the model can be used to analyse the cortical bone stiffness tensor.

II. SIMPLIFIED MODEL OF THE MULTILAYER SYSTEM

The model consists of an anisotropic elastic homogeneous layer of thickness h sandwiched between two homogeneous inviscid acoustic fluids. The two fluids have identical density ρ_f and celerity c_f . The elastic layer is characterized by its mass density ρ and a stiffness tensor. In this work, the multilayer system is used to simulate experimental *in vivo* signals obtained with the so-called axial transmission technique.

The model geometry, the location of the acoustic source and receivers are shown in Fig. 1. The acoustic source is defined as a line source, placed inside Ω_1 , and parallel to \mathbf{e}_2 where $(\mathbf{e}_1, \mathbf{e}_2, \mathbf{e}_3)$ is an orthonormal basis for the space, \mathbf{e}_3 being normal to the fluid-solid interfaces. The wave field will be computed at each point \mathbf{x} of the multilayer system with coordinate denoted (x_1, x_2, x_3) in the reference Cartesian frame $\mathbf{R}(O, \mathbf{e}_1, \mathbf{e}_2, \mathbf{e}_3)$, where O is the origin placed on interface Σ_1 .

The upper fluid layer (domain Ω_1) represents skin, muscle and echographic gel used in the experiment to ensure a good contact between the ultrasonic probe and the skin. The elastic layer (domain Ω) represents the cortical bone while the lower fluid layer (Ω_2) models the marrow. The thicknesses of the fluid layers Ω_1 and Ω_2 and of the elastic layer Ω are denoted h_1 , h_2 , and h respectively. Free boundary conditions are applied on top of the upper fluid layer (surface Γ_1) and bottom of the lower fluid layer (surface Γ_2). In this paper, attention is focused on the biomechanical variability of bone elasticity. Accordingly, the density and the stiffness tensor of the elastic layer are varying parameters of the model while all the other parameters have fixed values. The varying parameters are identified following the procedure described in section V.

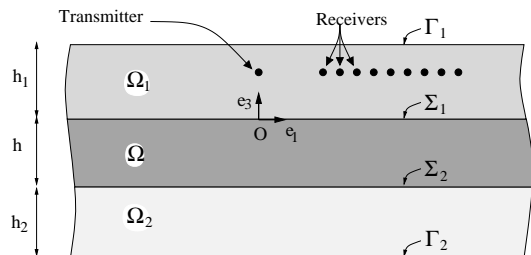


FIG. 1. Geometry of the multilayer system

III. PROBABILISTIC MODEL OF UNCERTAINTIES FOR THE ELASTICITY MATRIX OF THE SOLID LAYER

This section is devoted to the construction of a probabilistic model of the elastic material constituting the solid layer. The model accounts for uncertainties of the elastic constants in the bone material. That is, the bone elasticity is described by a mean stiffness tensor (with a prescribed symmetry: transverse isotropy in the paper) to which a random fluctuation is superimposed. Let c_{ijkh}

be the components of the mean elasticity tensor on basis $(\mathbf{e}_1, \mathbf{e}_2, \mathbf{e}_3)$. Then, mean elasticity matrix is defined as

$$[C] = \begin{pmatrix} [\tilde{C}_1] & [\tilde{C}_2] \\ [\tilde{C}_3] & [\tilde{C}_4] \end{pmatrix},$$

in which

$$[\tilde{C}_1] = \begin{pmatrix} c_{1111} & c_{1122} & c_{1133} \\ c_{2211} & c_{2222} & c_{2233} \\ c_{3311} & c_{3322} & c_{3333} \end{pmatrix},$$

$$[\tilde{C}_2] = \begin{pmatrix} \sqrt{2}c_{1123} & \sqrt{2}c_{1131} & \sqrt{2}c_{1112} \\ \sqrt{2}c_{2223} & \sqrt{2}c_{2231} & \sqrt{2}c_{2213} \\ \sqrt{2}c_{3323} & \sqrt{2}c_{3331} & \sqrt{2}c_{3312} \end{pmatrix},$$

$$[\tilde{C}_3] = \begin{pmatrix} \sqrt{2}c_{2311} & \sqrt{2}c_{2322} & \sqrt{2}c_{2333} \\ \sqrt{2}c_{3111} & \sqrt{2}c_{3122} & \sqrt{2}c_{3133} \\ \sqrt{2}c_{1211} & \sqrt{2}c_{1222} & \sqrt{2}c_{1233} \end{pmatrix},$$

$$[\tilde{C}_4] = \begin{pmatrix} 2c_{2323} & 2c_{2331} & 2c_{2312} \\ 2c_{3123} & 2c_{3131} & 2c_{3112} \\ 2c_{1223} & 2c_{1231} & 2c_{1212} \end{pmatrix}.$$

It should be noted that $[C_3] = [C_2]^T$. The construction of the probabilistic model consists in substituting $[C]$ by a random matrix $[\mathbf{C}]$ for which the probability density function is constructed using the information theory (see Shannon (1948, 1997)) with the available information defined as follows: (1) the random matrix $[\mathbf{C}]$ is a second-order random variable with values in the set $\mathbb{M}^+(\mathbb{R})$ of all the (6×6) real symmetric positive-definite matrices; (2) the mean value of random matrix $[\mathbf{C}]$ is the mean elasticity matrix $[C]$; (3) the norm of the inverse matrix of $[\mathbf{C}]$ is a second-order random variable. It has been shown in Soize (2001, 2005) that the random matrix $[\mathbf{C}]$ can then be written as

$$[\mathbf{C}] = [L]^T [\mathbf{G}] [L], \quad (1)$$

in which the (6×6) upper triangular matrix $[L]$ corresponds to the Cholesky factorization $[C] = [L]^T [L]$ and where the probability density function $p_{[\mathbf{G}]}$ of random matrix $[\mathbf{G}]$ is written as

$$p_{[\mathbf{G}]}([G]) = \mathbb{1}_{\mathbb{M}^+(\mathbb{R})}([G]) c (\det[G])^b \exp\{-a \text{tr}[G]\}, \quad (2)$$

where $a = 7/(2\delta^2)$, $b = a(1 - \delta^2)$, $\mathbb{1}_{\mathbb{M}^+(\mathbb{R})}([G])$ is equal to 1 if $[G]$ belongs to $\mathbb{M}^+(\mathbb{R})$ and is equal to zero if $[G]$ does not belong to $\mathbb{M}^+(\mathbb{R})$, $\text{tr}[G]$ is the trace of matrix $[G]$ and where positive constant c is such that

$$c = \frac{(2\pi)^{-15/2} a^{6a}}{\prod_{j=1}^6 \Gamma(\alpha_j)},$$

in which $\alpha_j = 7/(2\delta^2) + (1 - j)/2$ and where Γ is the Gamma function. The parameter δ allows the dispersion of the random matrix $[\mathbf{C}]$ to be controlled. Thus, the parameters of the probabilistic model of uncertainties for

the elasticity matrix are the components of $[C]$ and the coefficient δ . For such a probabilistic model, the random matrix $[\mathbf{G}]$ manifests the same statistical fluctuation in all its diagonal components and the same statistical fluctuation in all its extradiagonal components. It should be noted that the statistical fluctuations of the random matrix $[\mathbf{C}]$ are scaled with respect to the coefficients of the mean matrix $[C]$ (see Eq. (1)). One of the important aspects of the probabilistic model is that it takes into account any anisotropic fluctuation of the elasticity tensor. However, the components of random matrix $[\mathbf{C}]$ are statistically dependent real-valued random variables. The generator of the independent realizations of random matrix $[\mathbf{G}]$ according to its probability density function (Eq. (2)) is given in Appendix A.

IV. COMPUTATION OF THE RANDOM TRANSIENT WAVE RESPONSE

A. Solving the equations

The transient elasto-acoustic response of the multilayer fluid-solid system is computed in the time-domain with a fast and efficient hybrid solver (see Desceliers *et al.* (2008)). The symmetry of the problem allowed the previous problem to be reformulated in terms of the spatial coordinates x_1 and x_3 yielding a 2D-space boundary value problem. The solver is based on a time-domain formulation associated with a 1D-space Fourier transform for the infinite layer dimension (along the x_1 direction) and uses a finite element approximation in the direction perpendicular to the layers (along the x_3 direction). For a given mean elasticity matrix $[C]$, this solver allows the displacement field \mathbf{u} in Ω and the pressure fields p_1 and p_2 in Ω_1 and Ω_2 respectively, to be calculated. Consequently, there exist three mappings g_{p_1} , $g_{\mathbf{u}}$ and g_{p_2} such that

$$p_1(\mathbf{x}, t) = g_{p_1}(\mathbf{x}, t; [C]), \quad (3)$$

$$\mathbf{u}(\mathbf{x}, t) = g_{\mathbf{u}}(\mathbf{x}, t; [C]), \quad (4)$$

$$p_2(\mathbf{x}, t) = g_{p_2}(\mathbf{x}, t; [C]). \quad (5)$$

In addition, we introduce the von Mises stress at point $\mathbf{x} \in \Omega$ and at time t which is denoted by $\sigma^{\text{vm}}(\mathbf{x}, t)$. There also exists a mapping g_{vm} such that

$$\sigma^{\text{vm}}(\mathbf{x}, t) = g_{\text{vm}}(\mathbf{x}, t; [C]). \quad (6)$$

B. Velocity of the FAS and the axial transmission technique

The simulation of the actual measurements performed with the axial transmission technique consists in recording the signals $t \mapsto p_1(\mathbf{x}, t)$ at several receivers located in Ω_1 . The first arriving contribution of the signal (FAS) is considered. Following the signal processing method used with the experimental device the, velocity of FAS is determined from the time of flight of the first extremum of the contribution. Figure 2 shows a part of a simulated signal and the FAS. The simulated velocity v^{mod} of the

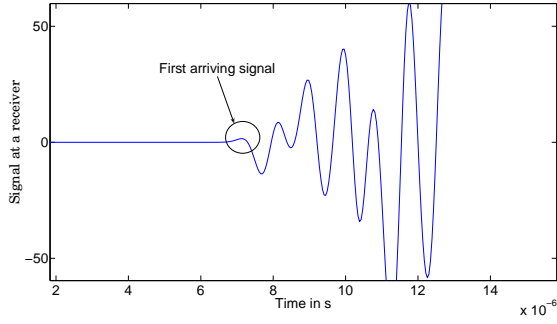


FIG. 2. Example of a signal at a receivers calculated by the model.

FAS is estimated based on the different time arrivals at the consecutive receivers. Consequently, there exists a mapping g_{velo} such that

$$v^{\text{mod}} = g_{\text{velo}}(p_1) \quad . \quad (7)$$

C. Random transient wave response and random velocity of the FAS

The transient elasto-acoustic response of the stochastic multilayer fluid-solid system is random. Accordingly, the pressure and displacements fields are modeled by three random fields P_1 , \mathbf{U} and P_2 indexed by $\Omega_1 \times [0, T_{\text{max}}]$, $\Omega \times [0, T_{\text{max}}]$ and $\Omega_2 \times [0, T_{\text{max}}]$ and with values in \mathbb{R} , \mathbb{R}^3 and \mathbb{R} respectively. Substituting the mean elasticity matrix $[C]$ by the random matrix $[\mathbf{C}]$ in Eqs. (3) to (5) yields

$$\begin{aligned} P_1(\mathbf{x}, t) &= g_{p_1}(\mathbf{x}, t; [\mathbf{C}]) \ , \\ \mathbf{U}(\mathbf{x}, t) &= g_{\mathbf{u}}(\mathbf{x}, t; [\mathbf{C}]) \ , \\ P_2(\mathbf{x}, t) &= g_{p_2}(\mathbf{x}, t; [\mathbf{C}]) \ . \end{aligned}$$

In addition, the velocity of the FAS and the von Mises stress are random variables denoted by V^{mod} and $\Sigma^{\text{vm}}(\mathbf{x}, t)$ respectively such that (see Eqs. (6) and (7))

$$\begin{aligned} \Sigma^{\text{vm}}(\mathbf{x}, t) &= g_{\text{vm}}(\mathbf{x}, t; [\mathbf{C}]) \ , \\ V^{\text{mod}} &= g_{\text{velo}}(P_1) \ . \end{aligned} \quad (8)$$

V. IDENTIFICATION PROCEDURE

The objective of this section is to present a method to identify all the parameters of the stochastic model from a database of *in vivo* signals obtained previously. The parameters to identify are the components $[C]_{ij}$ of the mean elasticity matrix $[C]$, the coefficient δ that controls the statistical fluctuations of random elasticity tensor and the mass density ρ .

A. Experimental database and random experimental velocity of the FAS

The *in vivo* measurements were previously performed on a population of 168 subjects examined at the third distal radius. This group is a subset of a larger group of patients who participated to a clinical evaluation of the bidirectional axial transmission device. The multi-element probe operating at a center frequency of 1 MHz recorded twenty series of axially transmitted signals without particular angular scanning protocol except natural micro-movements of the operator. The experimental database finally consisted of 2018 measurements of FAS velocity. Each velocity measurement is considered as a realization of a random variable V^{exp} corresponding to the random variable V^{mod} obtained with the stochastic simplified model. The mean value of V^{exp} is $v^{\text{exp}} = E\{V^{\text{exp}}\}$ and its coefficient of variation Δ^{exp} is defined by $(\Delta^{\text{exp}})^2 = E\{(V^{\text{exp}})^2\}/(v^{\text{exp}})^2 - 1$ in which $E\{\cdot\}$ is the mathematical expectation. Accordingly, the database consists of $N = 2018$ statistically independent realizations $V^{\text{exp}}(\hat{\theta}_1), \dots, V^{\text{exp}}(\hat{\theta}_N)$ of random variable V^{exp} . Using the usual statistical estimators and since N is sufficiently large, v^{exp} and Δ^{exp} can reasonably be estimated by

$$\begin{aligned} v^{\text{exp}} &= \frac{1}{N} \sum_{k=1}^N V^{\text{exp}}(\hat{\theta}_k) \ , \\ \Delta^{\text{exp}} &= \frac{1}{v^{\text{exp}}} \sqrt{\frac{1}{N} \sum_{k=1}^N V^{\text{exp}}(\hat{\theta}_k)^2 - (v^{\text{exp}})^2} \ . \end{aligned}$$

B. Optimization problem for the identification

For the identification, it is assumed that the mean elasticity matrix represents a transverse isotropic homogeneous medium. Then, all the components $[C]_{ij}$ are zeros except the following

$$\begin{aligned} [C]_{11} &= \frac{e_L^2(1 - \nu_T)}{(e_L - e_L\nu_T - 2e_T\nu_L^2)} \ , \\ [C]_{22} &= \frac{e_T(e_L - e_T\nu_L^2)}{(1 + \nu_T)(e_L - e_L\nu_T - 2e_T\nu_L^2)} \ , \\ [C]_{12} &= \frac{e_T e_L \nu_L}{(e_L - e_L\nu_T - 2e_T\nu_L^2)} \ , \\ [C]_{23} &= \frac{e_T(e_L\nu_T + e_T\nu_L^2)}{(1 + \nu_T)(e_L - e_L\nu_T - 2e_T\nu_L^2)} \ , \\ [C]_{44} &= g_T \ , \\ [C]_{55} &= g_L \ , \end{aligned}$$

with $[C]_{22} = [C]_{33}$, $[C]_{12} = [C]_{13} = [C]_{21} = [C]_{31}$, $[C]_{23} = [C]_{32}$ and $[C]_{55} = [C]_{66}$ and where (1) e_L and e_T are the longitudinal and transverse Young moduli, (2) g_L and g_T are the longitudinal and transversal shear moduli and (3) ν_L and ν_T are the longitudinal and transversal Poisson coefficients such that $g_T = e_T/2(1 + \nu_T)$. Consequently, for this case, the matrix $[C]$ is written as $[C] = [\chi(e_L, \nu_L, g_L, e_T, \nu_T)]$ in which the function

$[\chi]$ is completely defined. This equation shows that $[C]$ does not depend on 21 independent coefficients but only on 5 independent coefficients. Then, the parameters of the stochastic model which have to be identified would be the coefficients $e_L, \nu_L, g_L, e_T, \nu_T$, the mass density ρ and the coefficient δ . Let \mathbf{a} be the vector such that $\mathbf{a} = (\rho, e_L, \nu_L, g_L, e_T, \nu_T)$. The identification problem consists in finding vector \mathbf{a} and coefficient δ such that the stochastic model can represent the experimental database in a statistical sense. The optimal values $(\mathbf{a}^{\text{opt}}, \delta^{\text{opt}})$ for (\mathbf{a}, δ) is given by solving the following optimization problem

$$(\mathbf{a}^{\text{opt}}, \delta^{\text{opt}}) = \arg \min_{(\mathbf{a}, \delta)} F^{\text{cost}}(\mathbf{a}, \delta), \quad (9)$$

in which $F^{\text{cost}}(\mathbf{a}, \delta)$ is a cost function which has to be defined. The optimization problem defined by Eq. (9) is solved by the simplex algorithm (see Nelder and Mead (1965)). For each iteration of the simplex algorithm, the cost function has to be calculated which requires to solve the stochastic equations with Monte Carlo simulations (see Appendix A).

1. Cost function associated with the usual least-square approach

The cost function $F^{\text{cost}}(\mathbf{a}, \delta)$ associated with the usual least-square approach is defined as

$$F^{\text{cost}}(\mathbf{a}, \delta) = E\{(V^{\text{exp}} - V^{\text{mod}}(\mathbf{a}, \delta))^2\},$$

in which $V^{\text{mod}}(\mathbf{a}, \delta)$ is defined by Eq. (8) and where the dependance is \mathbf{a} and δ is written. It should be noted that V^{exp} and $V^{\text{mod}}(\mathbf{a}, \delta)$ are two independent random variables. Consequently, $F^{\text{cost}}(\mathbf{a}, \delta)$ can be rewritten as

$$F^{\text{cost}}(\mathbf{a}, \delta) = E\{(V^{\text{exp}} - v^{\text{exp}})^2\} + (v^{\text{exp}} - v^{\text{mod}}(\mathbf{a}, \delta))^2 + E\{(V^{\text{mod}}(\mathbf{a}, \delta) - v^{\text{mod}}(\mathbf{a}, \delta))^2\}, \quad (10)$$

in which $v^{\text{mod}}(\mathbf{a}, \delta) = E\{V^{\text{mod}}(\mathbf{a}, \delta)\}$. The first term in the right-hand side of Eq. (10) represents the variance of the random experimental velocity V^{exp} of the first arriving signal (which is independent of \mathbf{a} and δ). The second term in the right-hand side of Eq. (10) corresponds to the bias between the stochastic simplified model and the experimental system. The last term in the right-hand side of Eq. (10) is variance of the random velocity V^{mod} of the first arriving signal calculated with the stochastic simplified model. It should be noted that this variance is equal to zero if $\delta = 0$. Nevertheless, numerical experiments show that, for $\delta = 0$, it is always possible to find a value $\mathbf{a}_0^{\text{opt}}$ of parameter \mathbf{a} such that $v^{\text{exp}} - v^{\text{mod}}(\mathbf{a}, \delta) = 0$. Consequently, the usual least-square approach yields $\mathbf{a}^{\text{opt}} = \mathbf{a}_0^{\text{opt}}$ and $\delta^{\text{opt}} = 0$. Such a solution does not allow the statistical fluctuations due to uncertainties to be taken into account (because $\delta^{\text{opt}} = 0$) which proves that the cost function defined by Eqs. (10) is not adapted. This is the reason why a non usual cost function is introduced below.

2. Cost function adapted to the problem

We introduce a cost function F^{cost} which is more sensitive to the statistical fluctuations of the model, i.e. to the values of δ . Such a cost function is written as

$$F^{\text{cost}}(\mathbf{a}, \delta) = \frac{(v^{\text{exp}} - v^{\text{mod}}(\mathbf{a}, \delta))^2}{(v^{\text{exp}})^2} + \frac{(\Delta^{\text{exp}} - \Delta^{\text{mod}}(\mathbf{a}, \delta))^2}{(\Delta^{\text{exp}})^2},$$

in which

$$\Delta^{\text{mod}} = \sqrt{\frac{E\{(V^{\text{mod}}(\mathbf{a}, \delta))^2\}}{v^{\text{mod}}(\mathbf{a}, \delta)^2} - 1}.$$

This cost function is used for the optimization problem defined by Eq. (9) in order to identify the parameters \mathbf{a} and δ .

VI. RESULTS

A. Numerical data

The mean elasticity matrix of the cortical bone (layer Ω) is completely defined by the vector $\mathbf{a} = (\rho, e_L, \nu_L, g_L, e_T, \nu_T)$. The following numerical values for the components of \mathbf{a} are used (1) for the direct simulations presented in section VI.B and (2) as initial parameters for the optimization presented in section VI.C: $\rho = 1722 \text{ kg.m}^{-3}$, $e_L = 16.6 \text{ GPa}$, $\nu_L = 0.38$, $g_L = 4.7 \text{ GPa}$, $e_T = 9.5 \text{ GPa}$, $\nu_T = 0.44$, $g_T = 3.3 \text{ GPa}$, $\rho_f = 1000 \text{ kg.m}^{-3}$ and $c_f = 1500 \text{ m.s}^{-1}$. The acoustic line source is located at $x_1^S = 0$ and $x_3^S = 2 \times 10^{-3} \text{ m}$ and the time-history of the acoustic pulse is $F(t) = F_1 \sin(2\pi f_c t) e^{-4(t/f_c - 1)^2}$ where $f_c = 1 \text{ MHz}$ is the center frequency and $F_1 = 100 \text{ N}$.

B. Analysis of the propagation of the uncertainties

In this section, we present an analysis of the propagation of the uncertainties in the multilayer system with $h_1 = 10^{-2} \text{ m}$, $h = 4 \times 10^{-3} \text{ m}$ and $h_2 = 10^{-2} \text{ m}$. Firstly, the wave propagation of one realization of the system is analysed and clearly shows the effect of the anisotropy. Secondly, we analyse the mean value and the variance of the random wave propagation. This information allows the propagation of uncertainties to be quantified.

Let $[\mathbf{C}(\theta)]$ be one realization of the random elasticity matrix $[\mathbf{C}]$. For an elasticity matrix $[\mathbf{C}(\theta)]$, the realizations of the pressure fields in the two fluid media and the realization of the von Mises field in the solid medium are $P_1(\theta)$, $P_2(\theta)$ and $\Sigma^{\text{vm}}(\theta)$ and such that

$$\begin{aligned} P_1(\mathbf{x}, t; \theta) &= g_{p_1}(\mathbf{x}, t; [\mathbf{C}(\theta)]), \\ P_2(\mathbf{x}, t; \theta) &= g_{p_2}(\mathbf{x}, t; [\mathbf{C}(\theta)]), \\ \Sigma^{\text{vm}}(\mathbf{x}, t; \theta) &= g_{\text{vm}}(\mathbf{x}, t; [\mathbf{C}(\theta)]). \end{aligned}$$

Figures 3(a) to (h) show the graphs of the functions $(x_1, x_3) \mapsto P_1(x_1, x_3, t; \theta)$, $(x_1, x_3) \mapsto \Sigma^{\text{vm}}(x_1, x_3, t; \theta)$

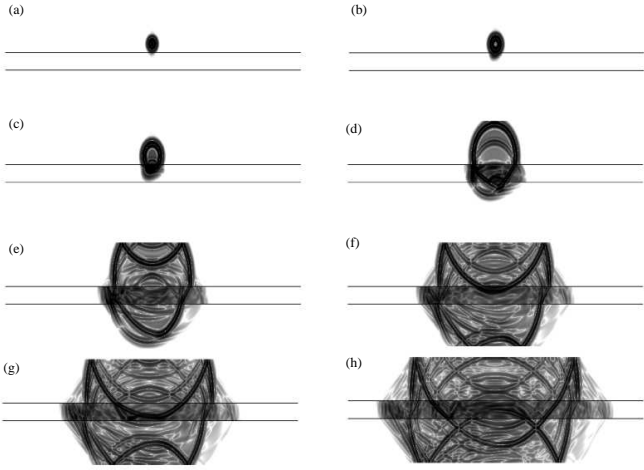


FIG. 3. Wave propagation in the three layers for a given realization of the random elasticity matrix at $t = 1.56 \mu s$ (a), $t = 2.06 \mu s$ (b), $t = 2.94 \mu s$ (c), $t = 5.89 \mu s$ (d), $t = 9.72 \mu s$ (e), $t = 13.55 \mu s$ (f), $t = 15.31 \mu s$ (g), $t = 119.88 \mu s$ (h).

and $(x_1, x_3) \mapsto P_2(x_1, x_3, t; \theta)$ at different time t . Let \underline{P}_1 , $\underline{\Sigma}^{\text{vm}}$ and \underline{P}_2 be the mean values of the stochastic fields P_1 , Σ^{vm} and P_2 . Figures 4(a) to (h) show the graphs of functions $(x_1, x_3) \mapsto \underline{P}_1(x_1, x_3, t)$, $(x_1, x_3) \mapsto \underline{\Sigma}^{\text{vm}}(x_1, x_3, t)$ and $(x_1, x_3) \mapsto \underline{P}_2(x_1, x_3, t)$ at different time t . Let var_{P_1} , $\text{var}_{\Sigma^{\text{vm}}}$ and var_{P_2} be the vari-

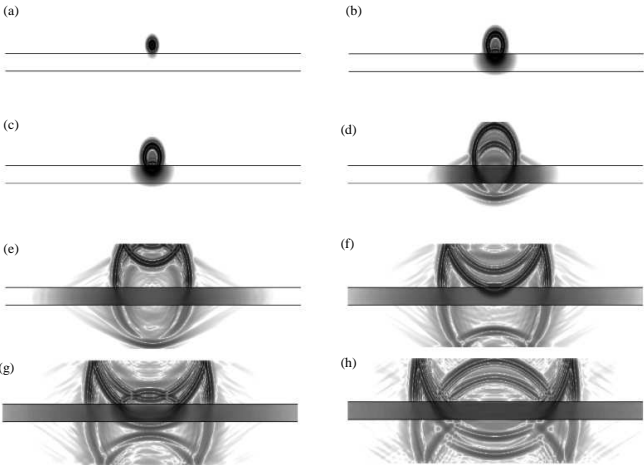


FIG. 4. Propagation of the mean waves in the three layers at $t = 1.56 \mu s$ (a), $t = 2.06 \mu s$ (b), $t = 2.94 \mu s$ (c), $t = 5.89 \mu s$ (d), $t = 9.72 \mu s$ (e), $t = 13.55 \mu s$ (f), $t = 15.31 \mu s$ (g), $t = 119.88 \mu s$ (h).

ances of the stochastic fields P_1 , Σ^{vm} and P_2 . Figures 5(a) to (h) show the graphs of the functions $(x_1, x_3) \mapsto \text{var}_{P_1}(x_1, x_3, t)$, $(x_1, x_3) \mapsto \text{var}_{\Sigma^{\text{vm}}}(x_1, x_3, t)$ and $(x_1, x_3) \mapsto \text{var}_{P_2}(x_1, x_3, t)$ at different time t .

The Figs. 3 to 5 taken together illustrate the stochastic wave propagation phenomenon. It can be seen in Fig. 3 that for one given realization, the wave field is particularly complex due the anisotropy: in Fig. 3 (which corre-

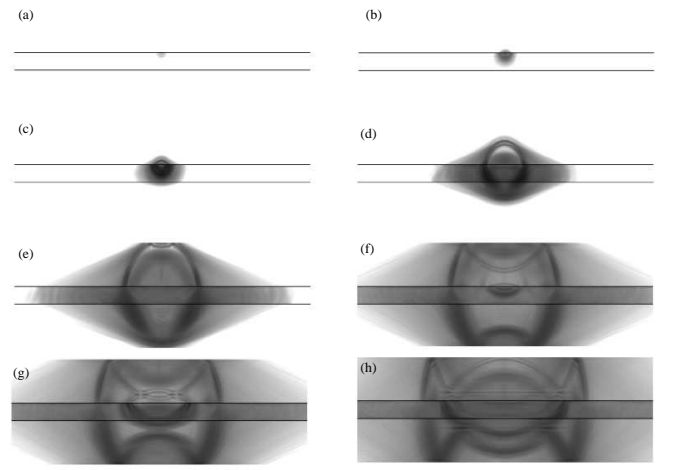


FIG. 5. Propagation of the uncertainties in the three layers at $t = 1.56 \mu s$ (a), $t = 2.06 \mu s$ (b), $t = 2.94 \mu s$ (c), $t = 5.89 \mu s$ (d), $t = 9.72 \mu s$ (e), $t = 13.55 \mu s$ (f), $t = 15.31 \mu s$ (g), $t = 119.88 \mu s$ (h).

sponds to a realization $[\mathbf{C}(\theta)]$ of the stiffness matrix with a relative strong deviation from transverse anisotropy) the complex anisotropy is in particular evidenced by the asymmetry with respect to (O, \mathbf{e}_3) of the wave field in the solid and in the bottom fluid layer. Such an asymmetry can be understood making use of slowness curves for anisotropic media (see for instance Royer and Dieulesaint (1999)): if the slowness curves happen to be asymmetric with respect \mathbf{e}_3 , the waves at the right and left of (O, \mathbf{e}_3) will travel at different velocities. In contrast, the mean and variance wave fields shown in Figs. 4 and 5 are quasi symmetric with respect to (O, \mathbf{e}_3) . This illustrates the fact that the anisotropic fluctuations of the stochastic elasticity matrix driven by δ do not have, on average, any preferential direction. Of course this can only be observed for the mean value and the variance. It should also be noted that the mean value of the different wave field realizations is not identical to the wave field obtained with the mean model unless $\delta = 0$ (i.e. no statistical fluctuation of the elasticity tensor). Figure 5 shows that there is a significant propagation of the uncertainties whose intensity is relative to the variances. Note that the upper wavefront in Figs. 3 and 4 corresponding to the direct cylindrical wave from the source is missing in Figs. 5 while the other waves which have interacted with the solid layer are observed. This is an illustration of the fact that the uncertainties in the wave propagation problem are associated to an interaction with the random elastic layer. Furthermore the intensity of the uncertainties is higher where the amplitude of the wave (close to the wave front) is higher. In addition, it can be deduced from the comparison of Figs. 4 and 5 that the dispersion coefficient of the wave propagation are not the same everywhere in the multilayer system.

C. Experimental validation of the stochastic model and identification of the model parameters

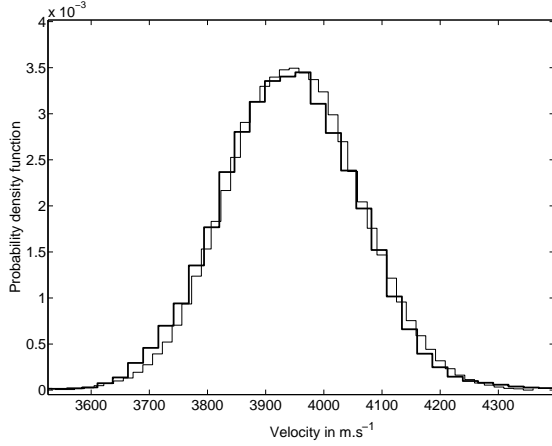


FIG. 6. Graph of the probability density function $v \mapsto p_{V^{\text{exp}}}(v)$ (thick solid lines) and graph of the density probability density functions $v \mapsto p_{V^{\text{mod}}}(v; \mathbf{a}^{\text{opt}}, \delta^{\text{opt}})$ with $\mathbf{a} = \mathbf{a}^{\text{opt}}$ and $\delta = \delta^{\text{opt}}$ (thin solid lines)

The identification of the vector $\mathbf{a} = (\rho, e_L, \nu_L, g_L, e_T, \nu_T)$ and the coefficient δ was carried out using the method presented in Section V with $h_1 = 2 \times 10^{-3}\text{m}$, $h = 4 \times 10^{-3}\text{m}$ and $h_2 = 10^{-2}\text{m}$. The solution $\mathbf{a}^{\text{opt}} = (\rho^{\text{opt}}, e_L^{\text{opt}}, \nu_L^{\text{opt}}, g_L^{\text{opt}}, e_T^{\text{opt}}, \nu_T^{\text{opt}})$ and δ^{opt} are such that $\rho^{\text{opt}} = 1598.8 \text{ kg.m}^{-3}$, $e_L^{\text{opt}} = 17.717 \text{ GPa}$, $\nu_L^{\text{opt}} = 0.3816$, $g_L^{\text{opt}} = 4.7950 \text{ GPa}$, $e_T^{\text{opt}} = 9.8254 \text{ GPa}$, $\nu_T^{\text{opt}} = 0.4495$ and $\delta^{\text{opt}} = 0.1029$. For $\mathbf{a} = \mathbf{a}^{\text{opt}}$ and $\delta = \delta^{\text{opt}}$, the realizations $V^{\text{mod}}(\mathbf{a}, \delta; \theta_1), \dots, V^{\text{mod}}(\mathbf{a}, \delta; \theta_N)$ of random velocity $V^{\text{mod}}(\mathbf{a}, \delta)$ are constructed with the stochastic simplified model and then, the probability density function $v \mapsto p_{V^{\text{mod}}}(v; \mathbf{a}, \delta)$ of $V^{\text{mod}}(\mathbf{a}, \delta)$ is estimated. Figure 6 shows in linear scale (1) the probability density function $v \mapsto p_{V^{\text{exp}}}(v)$ of the random variable V^{exp} estimated with $N = 2018$ experimental realizations $V^{\text{exp}}(\hat{\theta}_1), \dots, V^{\text{exp}}(\hat{\theta}_N)$; and (2) the probability density function $v \mapsto p_{V^{\text{mod}}}(v; \mathbf{a}^{\text{opt}}, \delta^{\text{opt}})$. The same data is plotted in Fig. 7 in logarithm scale in order to analyse the small levels of probabilities. These figures validate the stochastic simplified model in the statistical sense for the prediction of the velocity of the FAS.

VII. DISCUSSION AND CONCLUSIONS

A simplified elasto-acoustic multilayer model has been developed to simulate the ultrasonic wave propagation in a complex biomechanical system. In order to improve the simplified model, the uncertainties related to elastic behavior of the solid part have been taken into account using a probabilistic approach. The identification of the stochastic model parameters was conducted for *in vivo* data collected previously with an ultrasonic axial transmission device.

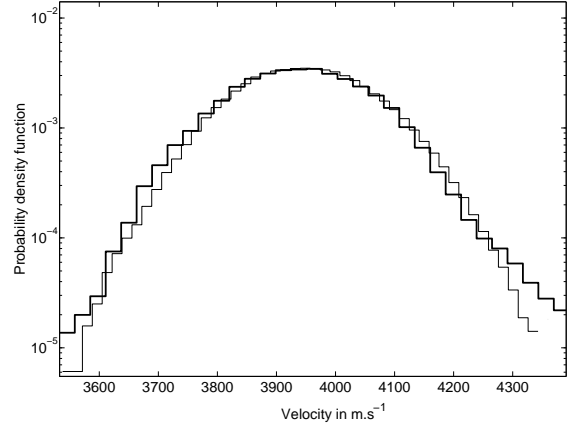


FIG. 7. Graphs of $v \mapsto \log(p_{V^{\text{exp}}}(v))$ (thick solid lines) and $v \mapsto \log(p_{V^{\text{exp}}}(v; \mathbf{a}^{\text{opt}}, \delta^{\text{opt}}))$ (thin solid lines).

Because the plots of the experimental and modeled probability density functions in Figs. 6 and 7 are so close, the stochastic simplified elasto-acoustic model is validated in the statistical sense regarding the prediction of the velocity of the FAS. Not only the mean value and the variance of the velocity are accurately predicted but also the experimental probability distribution is very well predicted; this remarkable result is not usual for such a complex system as that under consideration.

Furthermore, some values of the mean elastic constants of cortical bone and their fluctuations corresponding to the *in vivo* measurement database have been identified. As far as we know, the present work is the first attempt to identify the anisotropic elasticity tensor of cortical bone from actual measurement data. Note that the elastic parameter of the mean model which, after the optimization, is the most changed compared to the provided nominal elasticity values is the Young modulus e_L in the axial direction. This is consistent with the physics of the wave propagation associated with the FAS when the thickness is large compared to the wavelength: basically the velocity of the observed FAS tends to the velocity of a head wave initiated on the flat fluid- solid interface (see Bossy *et al.* (2002)) and which is associated to bulk longitudinal waves propagation in the solid.

However the identified elasticity values may not be compared straightforward to the actual bone elasticity values since they depend on the model configuration and on the fact that only the FAS contribution was considered. In the calculations, the thickness of the bone layer has been fixed among the largest physiological values; in these conditions, the FAS is known to be almost insensitive to the radius thickness (see Bossy *et al.* (2002)).

APPENDIX A: STOCHASTIC SOLVER

In this section, we present the stochastic solver that we have used to calculate the cost function F^{cost} . This stochastic solver is based on the Monte Carlo numerical

method. First, the generator of independent realizations of the random matrix $[\mathbf{G}]$ presented in Soize (2001, 2005) is used. Random matrix $[\mathbf{G}]$ is written $[\mathbf{G}] = [\mathbf{L}_G]^T [\mathbf{L}_G]$ in which $[\mathbf{L}_G]$ is a random upper triangular (6×6) real matrix whose random elements are independent variables defined as follow:

(1) For $j < j'$, the real-valued random variable $[\mathbf{L}_G]_{jj'}$ is written as $[\mathbf{L}_G]_{jj'} = \sigma U_{jj'}$ in which $\sigma = \delta / \sqrt{7}$ and where $U_{jj'}$ is a real-valued Gaussian random variable with zero mean and variance equal to 1.

(2) For $j = j'$, the positive-valued random variable $[\mathbf{L}_G]_{jj'}$ is written as $[\mathbf{L}_G]_{jj'} = \sigma \sqrt{2V_j}$ in which σ is defined above and where V_j is a positive-valued gamma random variable whose probability density function p_{V_j} with respect to dv is written as

$$p_{V_j}(v) = \mathbb{1}_{\mathbb{R}^+}(v) \frac{v^{(\gamma/(2\delta^2)+(1-j)/2)} e^{-v}}{\Gamma(\gamma/(2\delta^2) + (1-j)/2)} .$$

Then, n_s statistical independent realizations of random elasticity matrix $[\mathbf{C}]$ are constructed and are such that $[\mathbf{C}(\theta_1)] = [L]^T [\mathbf{G}(\theta_1)] [L], \dots, [\mathbf{C}(\theta_{n_s})] = [L]^T [\mathbf{G}(\theta_{n_s})] [L]$. Let $P_1(\theta_1), \dots, P_1(\theta_{n_s})$ be n_s statistical independent realizations of random field P_1 which are such that, for all $\mathbf{x} \in \Omega_1$ and $t \geq 0$, $P_1(\mathbf{x}, t; \theta_1) = g_{p_1}(\mathbf{x}, t; [\mathbf{C}(\theta_1)]), \dots, P_1(\mathbf{x}, t; \theta_{n_s}) = g_{p_1}(\mathbf{x}, t; [\mathbf{C}(\theta_{n_s})])$. As soon as the realizations of the random field P_1 are obtained, the realizations of the random velocity V^{mod} are deduced by $V^{\text{mod}}(\theta_1) = g_{\text{velo}}(P_1(\theta_1)), \dots, V^{\text{mod}}(\theta_{n_s}) = g_{\text{velo}}(P_1(\theta_{n_s}))$. For each value of \mathbf{a} and δ , the value of the cost function $F^{\text{cost}}(\mathbf{a}, \delta)$ is calculated by $F_{n_s}^{\text{cost}}$ (for sufficiently large values of n_s) such that

$$F_{n_s}^{\text{cost}} = \frac{(v^{\text{exp}} - v_{n_s}^{\text{mod}})^2}{(v^{\text{exp}})^2} + \frac{(\Delta^{\text{exp}} - \Delta_{n_s}^{\text{mod}})^2}{(\Delta_N^{\text{exp}})^2} ,$$

in which $v_{n_s}^{\text{mod}}$ and $\Delta_{n_s}^{\text{mod}}$ are the estimations of v^{mod} and Δ^{mod} defined as

$$v_{n_s}^{\text{mod}} = \frac{1}{n_s} \sum_{k=1}^{n_s} V^{\text{mod}}(\theta_k) ,$$

$$\Delta_{n_s}^{\text{mod}} = \frac{1}{v_{n_s}^{\text{mod}}} \sqrt{\frac{1}{n_s} \sum_{k=1}^{n_s} V^{\text{mod}}(\hat{\theta}_k)^2 - (v_{n_s}^{\text{mod}})^2} .$$

Bossy, E., Talmant, M., and Laugier, P., (2002) "Effect of bone cortical thickness on velocity measurements using ultrasonic axial transmission: A 2d simulation study", Journal of Acoustical Society of America, **112**(1), 297–307

Bossy, E., Talmant, M., Defontaine, M., Patat, F., and Laugier, P. (2004a) "Bidirectional axial transmission can improve accuracy and precision of ultrasonic velocity measurement in cortical bone: A validation on test materials", IEEE Trans. Ultrason. Ferroelectr. Freq. Control, **51**(1), 71–79

Bossy, E. , Talmant, M. , Laugier, P. (2004b), "Three-dimensional simulations of ultrasonic axial transmission velocity measurement on cortical bone models", J. Acoust. Soc. Am., **115**(5), 2314-2324

Bossy, E., Talmant, M., Peyrin, F., Akrou, L., Cloetens, P., and Laugier, P. (2004c), "An in vitro study of the ultrasonic axial transmission technique at the radius: 1-mhz velocity measurements are sensitive to both mineralization and intracortical porosity", J. Bone Miner. Res., **19**(9), 1548–1556

Camus, E; Talmant, M; Berger, G; *et al.* Analysis of the axial transmission technique for the assessment of skeletal status J. Acoust. Soc. Am., **108**(6), 3058-3065

Desceliers, C., Soize, C., Grimal, Q., Haiat, G., Naili, S. (2008), "A time-domain method to solve transient elastic wave propagation in a multilayer medium with a hybrid spectral-finite element space approximation", Wave Motion (in press)

Grimal, Q., Raum, K., Desceliers, C., Soize, C., Haiat, G., Naili, S., Talmant, M., and Laugier, P. (2007). "Stochastic simulation of the axial transmission technique based on a multi-scale model of bone material properties", in 2nd European Symposium on Ultrasonic Characterization of Bone. Halle, Germany: Aachen: Shaker Verlag.

Macocco, K. , Grimal, Q. , Naili, S., and Soize, C. (2006), "Elastoacoustic model with uncertain mechanical properties for ultrasonic wave velocity prediction: Application to cortical bone evaluation", J. Acoust. Soc. Am., **119**(2), 729–740

Nelder, J.A., Mead, R. (1965), "A simplex-method for function minimization", Computer Journal, **7**(4), 308-313

Raum, K., Leguerney, I., Chandelier, F., Bossy, E., Talmant, M., Saied, A., Peyrin, F., and Laugier, P. (2005), "Bone microstructure and elastic tissue properties are reflected in *qus* axial transmission measurements", Ultrasound in Medicine and Biology, **31**(9), 1225–1235.

Royer, D., and Dieulesaint, E. (1999) *Elastic waves in solids. Free and guided propagation*, Vol. 1, Springer Verlag.

Shannon, C.E. (1948) "A mathematical theory of communications", Bell System Technical Journal, **27**, 379–423

Shannon, C.E. (1997) "A mathematical theory of communications (reprinted)", M.D. Computing, **14**(4), 306–317

Soize, C. (2001), "Maximum entropy approach for modeling random uncertainties in transient elastodynamics", J. Acoust. Soc. Am., **109**(5), 1979–1996

Soize, C. (2005), "Random matrix theory for modeling uncertainties in computational mechanics", Computer Methods in Applied Mechanics and Engineering, **194**, 1333–1366